Journal of Computational Mathematics
Vol.28, No.3, 2010, 309–330.

http://www.global-sci.org/jcm
doi:10.4208/jcm.2009.10-m1015

ESTIMATOR COMPETITION FOR POISSON PROBLEMS*

C. Carstensen
Humboldt-Universität zu Berlin, Unter den Linden 6, 10099 Berlin, Germany
Department of Computational Science and Engineering, Yonsei University, 120-749 Seoul, Korea
Email: cc@math.hu-berlin.de
C. Merdon
Humboldt-Universität zu Berlin, Germany
Email: merdon@math.hu-berlin.de

Abstract

We compare 13 different a posteriori error estimators for the Poisson problem with lowest-order finite element discretization. Residual-based error estimators compete with a wide range of averaging estimators and estimators based on local problems. Among our five benchmark problems we also look on two examples with discontinuous isotropic diffusion and their impact on the performance of the estimators. (Supported by DFG Research Center MATHEON.)

Mathematics subject classification: 65N30, 65R20, 73C50.
Key words: Finite element methods, A posteriori error estimators.

1. Introduction

A posteriori error control has become an important issue for reliable and efficient computation of PDEs [1–6]. This paper updates the empirical study of [7] to modern a posteriori error control via the five classes of 13 estimators of Table 1.1 applied to the five benchmark examples of Table 1.2 such as the Poisson model problem on the L-shaped domain illustrated in Figure 1.1. Up to modified boundary conditions, marked by BC, all the benchmark problems are of the following type with or without discontinuous coefficients $\varkappa$ for some given right-hand side $f \in L^2(\Omega)$ and finite element approximation u_h to the unknown exact solution $u \in H^1_0(\Omega)$ of

$$\operatorname{div}(\varkappa \nabla u) + f = 0 \quad \text{in } \Omega. \tag{1.1}$$

Here and throughout the paper, $\Omega \subset \mathbb{R}^n$ is a bounded Lipschitz domain with Lebesgue and Sobolev spaces $L^2(\Omega)$ and $H^1(\Omega)$, and the piecewise constant diffusion coefficient $\varkappa$ is bounded by

$$0 < \varkappa_{\min} \leq \varkappa(x) \leq \varkappa_{\max} < \infty \quad \text{for all } x \in \overline{\Omega}. \tag{1.2}$$

By definition, an *error estimator* η is a computable quantity that aims to estimate the error $e := u - u_h$, e.g., in its energy norm,

$$|||e||| := \|\varkappa^{1/2} \nabla(u - u_h)\|_{L^2(\Omega)}.$$

* Received May 13, 2009 / Revised version received May 31, 2009 / Accepted June 6, 2009 / Published online February 1, 2010 /

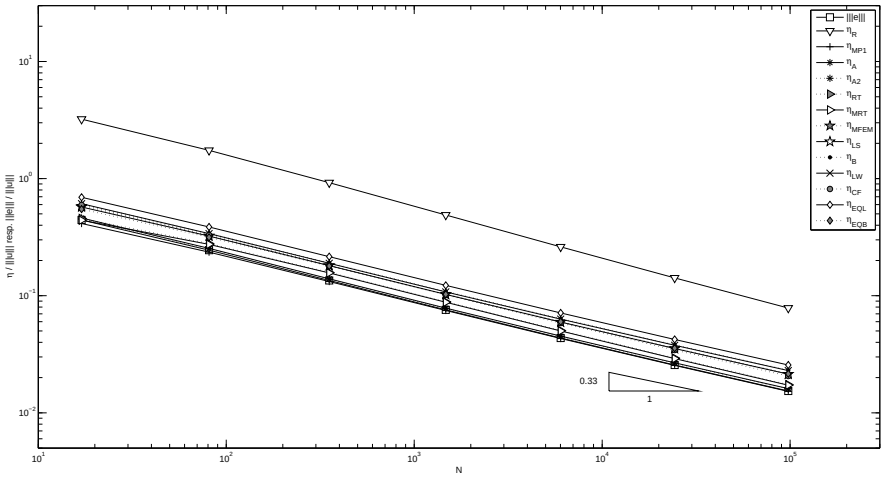

Fig. 1.1. Error and error estimators for uniform mesh refinement of L-shaped domain with right-hand side 1 from Example 7.1 in Section 7 to illustrate different accuracy of different error estimators.

Desirable properties of η are its *reliability* in the sense of an upper bound

$$|||e||| \leq \mathrm{C}_{\mathrm{rel}}\eta + \text{h.o.t.}$$

and its *efficiency* in the sense of a lower bound

$$\eta \leq \mathrm{C}_{\mathrm{eff}}|||e||| + \text{h.o.t.}$$

Any complete error control requires estimates of the constants $\mathrm{C}_{\mathrm{rel}}$ and $\mathrm{C}_{\mathrm{eff}}$ and the higher-order terms h.o.t. which are oscillations of the right-hand side f that are of magnitudes smaller than the energy error in all the examples of this paper. In many cases only the constant $\mathrm{C}_{\mathrm{rel}} = 1$ is known while $\mathrm{C}_{\mathrm{eff}}$ depends on generic constants [1, 3, 5].

We assume that $\mathcal{T}$ is a regular triangulation of Ω in the sense of Ciarlet [8,9] with nodes $\mathcal{N}$, free nodes $\mathcal{K} = \mathcal{N}\backslash\partial\Omega$ and edges $\mathcal{E}$ such that $\varkappa \in \mathcal{P}_0(\mathcal{T})$. The discrete space $\mathcal{P}_k(\mathcal{T})$ denotes the $\mathcal{T}$-piecewise polynomials of degree $\leq k$. The nodal basis function associated to $z \in \mathcal{N}$ is denoted

Table 1.1: Classes of a posteriori error estimators studied in this paper.

No	Class error estimators	Examples (Reference below)
1	explicit residual-based	η_{R} (Section 2)
2	averaging	η_{A1}, η_{A2}, η_{MP1}, η_{RT}, η_{MRT} (Section 3)
3	equilibration	η_{B}, η_{MFEM}, η_{LW}, η_{EQL}, η_{EQB} (Section 4)
4	least-square	η_{LS} (Section 4.2)
5	localisation	η_{CF} (Section 5)

Table 1.2: Benchmark examples studied in this paper.

No	Short name	Problem description in (1.1)	Feature
1	L-shaped domain	$\varkappa \equiv f \equiv 1$	corner singularity
2	Square domain	$\varkappa \equiv 1$, f with oscillations	oscillations
3	Slit domain	$\varkappa \equiv f \equiv 1$ & BC	slit singularity
4	Interface problem	jumping $\varkappa$, $f \equiv 0$ & BC	interface singularity
5	Octagon example	jumping $\varkappa$, $f \equiv 0$ & BC	continuous fluxes

by φ_z and its support by $\overline{\omega}_z$. Given the discrete solution $u_h \in \mathcal{S}_1(\mathcal{T}) := H^1_0(\Omega) \cap \mathcal{P}_1(\mathcal{T})$, its flux $\sigma_h = \varkappa \nabla u_h \in \mathcal{P}_0(\mathcal{T})$ and the exact counterpart $\sigma = \varkappa \nabla u$, we define the residual functional $\mathrm{Res} : H^1_0(\Omega) \longrightarrow \mathbb{R}$, for $v \in H^1_0(\Omega)$, by

$$\mathrm{Res}(v) := \int_\Omega (\sigma - \sigma_h) \cdot \nabla v \, dx = \int_\Omega f v \, dx - \int_\Omega \sigma_h \cdot \nabla v \, dx. \tag{1.3}$$

The identity $|||e||| = |||\mathrm{Res}|||_*$ leads to the estimation of the dual norm of Res. The most popular way to do this is via the standard residual-based a posteriori error estimator η_{R} [1, 3, 4, 10–13] which is relatively cheap but usually overestimates the error about a factor of ten or larger [7]. Therefore, more elaborate estimators are of interest, even if their calculation is more expensive.

For an arbitrary function $q \in H(\mathrm{div}; \Omega)$ an integration by parts shows

$$\mathrm{Res}(v) = \int_\Omega (f + \mathrm{div} q) v \, dx - \int_\Omega (\sigma_h - q) \cdot \nabla v \, dx, \tag{1.4}$$

a representation also suggested in [14]. The quantity q has the interpretation as an averaging or post-processing of σ_h and enables various designs of an error estimator, e.g., by piecewise affine $H(\mathrm{div}; \Omega)$-functions which form the discrete space of first-order averagings

$$Q_1(\mathcal{T}) := H(\mathrm{div}; \Omega) \cap \mathcal{P}_1(\mathcal{T})^n$$

which includes $\mathcal{S}_1(\mathcal{T})^n$ as well as the Raviart-Thomas finite element space

$$RT_0(\mathcal{T}) := \Big\{ q \in L^2(\Omega; \mathbb{R}^n) \ : \ \exists a \in \mathcal{P}_0(\mathcal{T})^n, \exists b \in \mathcal{P}_0(\mathcal{T}) \text{ s.t.} \\ q(x) = a + bx \text{ for a.e. } x \in \Omega \text{ and } [q \cdot \nu_E] = 0 \text{ on all inner edges } E \Big\}.$$

Given $q \in Q_1(\mathcal{T})$ the quantity

$$\eta(q) := \|\varkappa^{-1/2}(\sigma_h - q)\|_{L^2(\Omega)}$$

can be shown to be reliable and so, for any interpolation operator

$$\mathcal{A} : \ H(\mathrm{div}; \Omega) \longrightarrow Q_1(\mathcal{T}),$$

the value $\eta_{\mathcal{A}} = \eta(\mathcal{A}(\sigma))$ is a reliable estimator: All averaging is reliable [15]. Minimizing $\eta(q)$ over $q \in \mathcal{S}_1(\mathcal{T})^n$ gives the estimator η_{MP1} with

$$\begin{aligned} \eta_{\mathrm{MP1}} &:= \min_{q \in \mathcal{S}_1(\mathcal{T})^n} \|\varkappa^{-1/2}(\sigma_h - q)\|_{L^2(\Omega)} \\ &\le |||e||| + \min_{q \in \mathcal{S}_1(\mathcal{T})^n} \|\varkappa^{-1/2}(\sigma - q)\|_{L^2(\Omega)}. \end{aligned}$$

In case $\varkappa \equiv 1$ and smooth exact solution the latter term is of higher order. In the numeric experiments, the estimator η_{MP1} shows surprisingly accurate results. However, when it comes to discontinuities in $\varkappa$, an ansatz with globally continuous functions appears less accurate. In that case, the exact flux σ could have tangential jumps over interfaces of neighbouring domains with constant diffusion. A more promising ansatz is the use of Raviart-Thomas elements $q \in RT_0(\mathcal{T})$ for which the normal jumps $[q \cdot \nu_E]$ vanishes while the tangential jumps are a priori unrestricted. A minimisation of $\eta(q)$ for $q \in RT_0(\mathcal{T})$ yields the estimator

$$\eta_{\mathrm{MRT}} := \min_{q \in RT_0(\mathcal{T})} \|\varkappa^{-1/2}(\sigma_h - q)\|_{L^2(\Omega)}.$$

Efficiency of $\eta_{\rm MRT}$ follows from that of the estimator $\eta_{\rm RT} := \eta(q_{\rm RT}) \geq \eta_{\rm MRT}$ where the normal flux of $q_{\rm RT} \in RT_0(\mathcal{T})$ on an edge $E \in \mathcal{E}$ is chosen as the arithmetic average $< \sigma_h \cdot \nu_E >$ of the normal fluxes of σ_h on both sides of the edge.

To obtain estimators with a secure reliable constant $\mathrm{C}_{\rm rel} = 1$ we can design q such that it fullfills an equilibration condition of the form

$$\mathrm{div} q = -Pf, \tag{1.5}$$

where Pf is a suitable interpolation of f, such that the first term in (1.4) becomes negligible or raises oscillations. This depends on the chosen approximation space for q. In case of $q \in RT_0(\mathcal{T})$ the $\mathcal{T}$-piecewise mean value $f_{\mathcal{T}} \in \mathcal{P}_0(\mathcal{T})$ of f defines the oscillation term

$$\mathrm{osc}(f, \mathcal{T}) = \|h_{\mathcal{T}}(f - f_{\mathcal{T}})\|_{L^2(\Omega)}, \tag{1.6}$$

which is expected to be of higher order for $f \in H^1(\Omega)$. In fact, all examples of this paper are not dominated by the osciallations and undisplayed numerical experiments show that they stay much smaller than the other estimator contributions.

We will mention five design ways for q, among them are a least-square approach similar to [6,16], solving the dual mixed problem [17,18] and three methods based on local problems on node patches for determination of equilibrated fluxes. The one suggested by Luce and Wohlmuth [19] utilizes the dual mesh, while the algorithm by Braess [11,20] computes a correction for σ_h composed of overlapping broken Raviart-Thomas elements. The output of the last method by Ladeveze and Leguillon matches the equilibration condition only in a weak sense which is still enough to set up and solve local Neumann problems and obtain the estimator $\eta_{\rm EQ}$ from [1].

The remaining part of the paper is organized as follows. Section 2 introduces the explicit residual-based-estimator and its modification for the case of discontinuous diffusion [21]. Section 3 discusses estimators using first-order averagings. Section 4 introduces the estimators based on the equilibration condition (1.5) to obtain estimators with $\mathrm{C}_{\rm rel} = 1$. For comparison, we added the local problem estimator $\eta_{\rm CF}$ from [22] in Section 5. Section 6 introduces the adaptive mesh refinement strategy used for the five examples in Section 7. Some observations from the experimental results in Section 8 conclude this paper.

2. Residual-based a Posteriori Error Estimates

This section is devoted to the definition of the explicit residual-based error estimator on a regular triangulation $\mathcal{T}$ of the Lipschitz domain $\Omega \subset \mathbb{R}^2$ into triangles. Recall that $\mathcal{N}$ and $\mathcal{E}$ denotes the nodes and edges of the triangulation. Furthermore, $\varkappa_T$ denotes the value of $\varkappa$ on $T \in \mathcal{T}$ and $\varkappa_E := \max_{T \in \mathcal{T}, E \subset \partial T} \varkappa_T$ for $E \in \mathcal{E}$.

Definition 2.1. *For $T \in \mathcal{T}$ define*

$$\eta_{R,T}^2 := \frac{h_T^2}{\varkappa_T} \|f\|_{L^2(T)}^2 + \sum_{E \subset \partial T} \frac{h_E}{\varkappa_E} \|[\sigma_h \cdot \nu_E]\|_{L^2(E)}^2,$$

and globally

$$\eta_R := \left(\sum_{T \in \mathcal{T}} \frac{h_T^2}{\varkappa_T} \|f\|_{L^2(T)}^2 \right)^{1/2} + \left(\sum_{E \in \mathcal{E}} \frac{h_E}{\varkappa_E} \|[\sigma_h \cdot \nu_E]\|_{L^2(E)}^2 \right)^{1/2}.$$

The estimator η_{R} is known to be reliable and efficient.

Theorem 2.1. ([22]) *If $n = 2$, $\varkappa \equiv 1$ and $\mathcal{T}$ consists of right isosceles triangles, it holds*

$$|||e||| \leq \eta_R.$$

In case of $\varkappa \not\equiv 1$ the constant $\mathrm{C}_{\mathrm{rel}}$ depends on the global bound $\varkappa_{\max}/\varkappa_{\min}$. This dependency is eliminated if $\varkappa$ is distributed quasimonotone, i.e., $\varkappa$ assumes at most one local maximum around each node. At boundary nodes, every element with a local maximum must touch the boundary, cf. [23] for details. The point is that this property allows to travel from one element of the node patch to (the) one with the largest number on a monotonous path. The reliability proof is based on an interpolation operator $\mathcal{I}_\varkappa$ with the properties

$$\begin{aligned} \|v - \mathcal{I}_\varkappa(v)\|_{L^2(T)} &\leq c_1 h_T \varkappa_T^{-1/2} |||v|||_{(U_T)} \quad \text{for all } T \in \mathcal{T}, \\ \|v - \mathcal{I}_\varkappa(v)\|_{L^2(E)} &\leq c_2 h_E^{1/2} \varkappa_E^{-1/2} |||v|||_{(U_E)} \quad \text{for all } E \in \mathcal{E}\backslash\partial\Omega. \end{aligned}$$

Here, U_T and U_E denote sufficently large neighbourhoods of T and E respectively. Then $\mathrm{C}_{\mathrm{rel}}$ of η_{R} depends on the constants c_1 and c_2 which (in case of quasimononotony) do neighter depend on the local mesh-size nor on the global bounds of $\varkappa$. The efficiency constant $\mathrm{C}_{\mathrm{eff}}$ of η_{R} does not depend on the global bounds of $\varkappa$ also in the non-quasimonotone case [21].

3. Averaging Estimators

Recall that

$$Q_1(\mathcal{T}) := H(\mathrm{div}; \Omega) \cap \mathcal{P}_1(\mathcal{T})^n$$

denotes the space of first-order averagings, i.e., piecewise affine $H(\mathrm{div}; \Omega)$-functions. We prove that $q \in Q_1(\mathcal{T})$ generates a reliable estimator. For this we need an interpolation operator

$$\mathcal{I} : H_0^1(\Omega) \longrightarrow \mathcal{S}_1(\mathcal{T})$$

with stability, first-order approximation, and orthogonality properties

$$\|h_{\mathcal{T}}^{-1} \varkappa^{1/2} (v - \mathcal{I}(v))\|_{L^2(\Omega)} \leq c_3 |||v|||, \tag{3.1}$$

$$|||v - \mathcal{I}(v)||| \leq c_4 |||v|||, \tag{3.2}$$

$$\int_\Omega f(v - \mathcal{I}(v))\, dx \leq c_5 \mathrm{osc}(f, \mathcal{T}) |||v|||. \tag{3.3}$$

Such operators exist [24] with constants c_3, c_4, c_5 which depend on the global eigenvalue bounds $\varkappa_{\min}$ and $\varkappa_{\max}$ of $\varkappa$. For the quasimonotone case it is possible to design operators with constants c_3, c_4, c_5 that are independent of $\varkappa_{\min}$ and $\varkappa_{\max}$. The aforementioned operator $\mathcal{I}_\varkappa$ of Bernardi and Verfuerth from [21] certainly has the first property but possibly lacks the others. A suitable modification of the operator from [24] is designed in [25] where the third property is replaced by another but similar one. The point is that the third property has to raise oscillations or so.

Theorem 3.1. *Let $\mathcal{I}$ be an interpolation operator with the properties* (3.1)-(3.3). *Then for $q \in Q_1(\mathcal{T})$ it holds*

$$|||\mathrm{Res}|||_* \leq (c_4 + c_3 c_6)\eta(q) + c_5 \mathrm{osc}(f, \mathcal{T}).$$

Proof. Eq. (1.4) and Galerkin orthogonality show

$$\mathrm{Res}(v) = \int_\Omega (f + \mathrm{div} q)(v - \mathcal{I}(v))dx - \int_\Omega (\sigma_h - q)\cdot\nabla(v - \mathcal{I}(v))dx.$$

A Cauchy inequality in the latter term is combined with property (3.2) to obtain

$$\int_\Omega (\sigma_h - q)\cdot\nabla(v - \mathcal{I}(v))dx \le c_4\eta(q)|||v|||.$$

For the first term we use properties (3.1) and (3.3) which results in

$$\begin{aligned}&\int_\Omega (f + \mathrm{div} q)(v - \mathcal{I}(v))dx\\ \le&|||v||| \left(c_5\mathrm{osc}(f,\mathcal{T}) + c_3\|h_{\mathcal{T}}\varkappa^{-1/2}\mathrm{div} q\|_{L^2(\Omega)}\right).\end{aligned}$$

An elementwise inverse estimate for polynomials (notice that $\mathrm{div}_{\mathcal{T}}\sigma = 0$) of the form

$$\|h_{\mathcal{T}}\varkappa^{-1/2}\mathrm{div}_{\mathcal{T}}(q - \sigma_h)\|_{L^2(T)} \le c_6\|\varkappa^{-1/2}(q - \sigma_h)\|_{L^2(T)}$$

yields

$$\|h_{\mathcal{T}}\varkappa^{-1/2}\mathrm{div} q\|_{L^2(\Omega)} \le c_6\eta(q).$$

This completes the proof of the theorem. □

The following five choices for q and their numerical performance is discussed in section 7:

- $\eta_{\mathrm{A1}} = \eta(q_1)$ with
$$q_1 := \sum_{z\in\mathcal{N}} \varphi_z \fint_{\omega_z} \sigma_h\, dx,$$
- $\eta_{\mathrm{A2}} = \eta(q_2)$ with
$$q_2 := \sum_{z\in\mathcal{N}} \varphi_z \lim_{r\to 0^+} \fint_{B(z,r)\cap\Omega} \sigma_h\, dx,$$
- $\eta_{\mathrm{RT}} = \eta(q_{\mathrm{RT}})$ with $q_{\mathrm{RT}} \in RT_0(\mathcal{T})$ and $q_{\mathrm{RT}}\cdot\nu_E =< \sigma_h\cdot\nu_E >$,
- $\eta_{\mathrm{MP1}} = \eta(q_{\mathrm{MP1}}) = \min_{q\in\mathcal{S}_1(\mathcal{T})^n}\eta(q)$,
- $\eta_{\mathrm{MRT}} = \eta(q_{\mathrm{MRT}}) = \min_{q\in RT_0(\mathcal{T})}\eta(q)$.

Remark 3.1.

(a) The local refinement indicators for $T \in \mathcal{T}$ for the adaptive mesh generation are generated by restricting the norm in $\eta(q)$ on T.

(b) A discrete norm equivalence for (broken) Raviart-Thomas function $r \in RT_{-1}(T)$ yields

$$\|\varkappa^{-1/2}r\|_{L^2(T)} \approx \sum_{E\subset\partial T} h_E^{1/2}/\varkappa_T^{1/2}\|r\cdot\nu_E\|_{L^2(E)}.$$

Replacing r by $\sigma_h - \hat{q}$ this shows equivalence of η_{RT} and the edge contribution of η_{R2} and therefore efficiency for η_{MRT} and η_{RT}.

(c) Efficiency for η_{MP1} is known for smooth exact solution and globally constant $\varkappa$ [15], but cannot be guaranteed in the discontinous case as we will also see in the numerical examples.

(d) Averaging techniques were proposed by engineers [26]; their general reliability was first indicated by [12, 13] by dominating edge contributions [24, 27, 28], cf. also [29, 30].

(e) The observation that *all averaging estimators are reliable* is due to [31] and studied in [32] for higher order finite element schemes, in [33, 34] for elasticity and the Stokes equation, and eventually in [35, 36] for variational inequalities.

4. Equilibration Estimators

To obtain a secure upper bound of the error we introduce several constructions that fullfill an equilibration condition of the form

$$\mathrm{div} q = -Pf.$$

4.1. Equilibration after Braess

The idea of Braess [11, 20] is to construct a Raviart-Thomas element $q \in RT_0(\mathcal{T})$ with $Pf = f_{\mathcal{T}}$, where $f_{\mathcal{T}}$ is the $\mathcal{T}$-piecewise constant integral mean of f. Utilizing the $\mathcal{P}_0(\mathcal{T})$-orthogonality of $f - f_{\mathcal{T}}$ and the Poincaré inequality this yields for every $v \in H^1(\Omega)$

$$\begin{aligned}\int_\Omega (f + \mathrm{div} q) v\, dx &= \int_\Omega (f - f_{\mathcal{T}}) v\, dx \\ &= \sum_{T\in\mathcal{T}} \int_T (f - f_{\mathcal{T}})(v - v_{\mathcal{T}})\, dx \\ &\le \sum_{T\in\mathcal{T}} h_T/\pi \|f - f_{\mathcal{T}}\|_{L^2(T)} \|\nabla v\|_{L^2(T)} \\ &\le \sum_{T\in\mathcal{T}} h_T/\pi \|\varkappa^{-1/2}(f - f_{\mathcal{T}})\|_{L^2(T)} \|\varkappa^{1/2}\nabla v\|_{L^2(T)} \\ &\le 1/\pi\ \mathrm{osc}(f/\varkappa^{1/2}, \mathcal{T}) |||v||| \end{aligned} \tag{4.1}$$

Finally the Cauchy inequality in the last term of (1.4) gives

$$\begin{aligned}&\int_\Omega (\sigma_h - q)\cdot \nabla v\, dx \\ &= \int_\Omega \varkappa^{-1/2}(\sigma_h - q)\cdot(\varkappa^{1/2}\nabla v) dx \le \eta(q) |||v|||\end{aligned} \tag{4.2}$$

and leads to

$$|||\mathrm{Res}|||_* \le \eta(q) + 1/\pi\ \mathrm{osc}(f/\varkappa^{1/2}, \mathcal{T}).$$

The construction by Braess works by calculating a correction $r \in RT_{-1}(\mathcal{T})$ that eliminates the jumps of σ such that $q_{\mathrm{B}} := \sigma_h + r$ has the desired properties. The correction r is decomposed into the sum of broken Raviart-Thomas elements over node patches $r_z \in RT_{-1}(\mathcal{T}_{|\omega_z})$ with

$$\mathrm{div} r_z = -(\varphi_z f)_{\mathcal{T}}, \qquad r_z \cdot \nu_E = 0 \text{ on } \partial\omega_z \backslash \partial\Omega \qquad \text{and} \qquad [r_z \cdot \nu_E] = -1/n\ [\sigma_h \cdot \nu_E]$$

for all edges $E \in \mathcal{E}\backslash\partial\Omega$ with $z \in E$. Each r_z can be calculated independently by determination of the remaining nonzero normal fluxes of r_z on the elements of the patch. The associated estimator will be labeled with $\eta_{\rm B} := \eta(q_{\rm B}) = \|\varkappa^{-1/2} r\|_{L^2(\Omega)}$.

The minimum

$$\eta_{\rm MFEM} = \eta(q_{\rm MFEM}) = \inf_{\substack{q \in RT_0(\mathcal{T}) \\ {\rm div} q = -f_{\mathcal{T}}}} \eta(q)$$

is known to be attained in the gradient part of the solution of the dual mixed formulation of (1.1) with Raviart-Thomas elements of lowest order [11, 17, 18].

4.2. Least-Square-Estimator

Following ideas in [16] we use the Friedrichs inequality after separating the oscillations (4.1) to obtain

$$\begin{aligned}\int_\Omega (f + {\rm div} q) v\, dx &= \int_\Omega (f - f_{\mathcal{T}}) \cdot v\, dx + \int_\Omega (f_{\mathcal{T}} + {\rm div} q) v\, dx \\ &\leq \Big({\rm osc}(f/\varkappa^{1/2}, \mathcal{T})/\pi + C_F/\varkappa_{\rm min}^{1/2} \|f_{\mathcal{T}} + {\rm div} q\|_{L^2(\Omega)} \Big) \, |||v|||\end{aligned}$$

and determine

$$\eta_{\rm LS}^2 = \eta(q_{\rm LS})^2 = \inf_{q \in RT_0(\mathcal{T})} \Big(\eta(q)^2 + 1/\varkappa_{\rm min} \|f_{\mathcal{T}} + {\rm div} q\|_{L^2(\Omega)}^2 \Big) .$$

It certainly holds $\eta_{\rm MRT} \leq \eta_{\rm LS} \leq \eta_{\rm MFEM} \leq \eta_{\rm B}$. The second term $f_{\mathcal{T}} + {\rm div} q$ doesn't depend on the mesh size, hence it must converge against zero since otherwise it cannot be efficient. That's why we expect $\eta_{\rm LS}$ to coincide with $\eta_{\rm MFEM}$ asymptotically. However, it may deliver better results in the pre-asymptotic range. Reliability depends on knowledge of the constant $C_F \leq {\rm diam}(\Omega)/\pi$. This led Repin to the guaranteed upper bound (he called majorant)

$$|||e||| \leq \inf_{q \in Q_h} \Big(\eta(q) + C_F \|f + {\rm div} q\|_{L^2(\Omega)} \Big),$$

which follows from the Friedrichs inequality in (1.4) and ignores the possible refinement by oscillations. The elementwise contributions of $\eta(\overline{q})$ to the minimizer $\overline{q} \in Q_h$ serve as refinement indicators. Here, Q_h is *any* finite-dimensional subspace of $H({\rm div}; \Omega)$, e.g. $RT_0(\mathcal{T})$ as in the other estimators. The accuracy is increased by means of using higher-order elements for q locally where f is oscillating or relatively large. However, our suggestion is to separate oscillations (or any other other $f - Pf$ that raises oscillations and fullfills $Pf \in {\rm div} Q_h$) already in the variational state of the derivation. This leads to the recommendation of other estimators in Subsection 8.8.

4.3. Equilibration after Luce and Wohlmuth

The technique by Luce and Wohlmuth [19] generates a Raviart-Thomas element $q_{\rm LW}$ on a refined triangulation achieved by connecting the nodes and edge midpoints (and face midpoints) of each element with its center. In that way every element is devided into $(n+1)!$ elements with same area. All child-elements sharing the same node z form a polygonial K_z which is a member of the dual mesh. By setting $q \cdot \nu_e = \sigma_h \cdot \nu_e$ for inter-polygonial boundaries e (where

the normal flux of σ is continuous) only the fluxes inside the polygonials remain unknown and can be determined independently on each polygonial K_z, $z \in \mathcal{N}$ such that the equilibration condition

$$\mathrm{div} q_{\mathrm{LW}} = -1/|K_z| \int_{\omega_z} f\varphi_z \, dx$$

holds. This choice of Pf also yields terms of higher order or oscillations for the first term in (1.4). The associated estimator reads $\eta_{\mathrm{LW}} := \eta(q_{\mathrm{LW}}) = \|\varkappa^{-1/2}(\sigma - q_{\mathrm{LW}})\|_{L^2(\Omega)}$.

4.4. Equilibration after Ladeveze and Leguillon

This subsection is devoted to the equilibration estimator due to Ladeveze and Leguillon [1, 37–40] in the implementation of [1].

Decomposing (1.4) over a sum of triangles and elementwise integration by parts yields (ν is the outer normal on ∂T)

$$\begin{aligned}
\mathrm{Res}(v) &= \sum_{T\in\mathcal{T}} \int_T (f + \mathrm{div} q) v \, dx - \int_T (\sigma_h - q) \cdot \nabla v \, dx \\
&= \sum_{T\in\mathcal{T}} \int_T f v \, dx - \int_T \sigma_h \cdot \nabla v \, dx + \int_{\partial T} q \cdot \nu v \, ds \\
&= \sum_{T\in\mathcal{T}} \mathrm{Res}_T(v, q)
\end{aligned}$$

with

$$\mathrm{Res}_T(v, q) := \int_T f v \, dx - \int_T \sigma_h \cdot \nabla v \, dx + \int_{\partial T} q \cdot \nu v \, ds. \tag{4.3}$$

We define the local function spaces $H^1_D(T)$ as $H^1(T)\backslash\mathbb{R}$ if $|T \cap \partial\Omega| = 0$ and otherwise as $\{v \in H^1(T) \,:\, v = 0 \ \text{ on } \partial T \cap \partial\Omega\}$.

Theorem 4.1. *Suppose* $\mathrm{Res}_T(1, q) = 0$ *for any* $T \in T$ *with* $|T \cap \partial\Omega| > 0$. *Then for all* $T \in \mathcal{T}$, *there exist a unique* $\phi_T \in H^1_D(T)$ *with*

$$\int_T \varkappa \nabla \phi_T \cdot \nabla v \, dx = \mathrm{Res}_T(v, q) \quad \text{ for all } v \in H^1_D(T). \tag{4.4}$$

Moreover (ϕ_T *denotes the solution of* (4.4)),

$$|||e||| \le \eta_{EQ} := \left(\sum_{T\in\mathcal{T}} \|\varkappa^{1/2} \nabla \phi_T\|^2_{L^2(T)} \right)^{1/2}. \tag{4.5}$$

Proof. The solvability of the local problems 4.4 is well known. The calculation in the beginning of this subsection shows

$$\begin{aligned}
\mathrm{Res}(v) &= \sum_{T\in\mathcal{T}} \mathrm{Res}_T(v, q) \\
&= \sum_{T\in\mathcal{T}} \int_T \varkappa \nabla \phi_T \cdot \nabla v \, dx \\
&\le \sum_{T\in\mathcal{T}} \|\varkappa^{1/2} \nabla \phi_T\|_{L^2(T)} \|\varkappa^{1/2} \nabla v\|_{L^2(T)} \\
&\le \eta_{\mathrm{EQ}} |||v|||.
\end{aligned}$$

□

Remark 4.1.

(a) For this ansatz it is actually enough to know the edge functionals $\mu_E := q \cdot \nu_E$. An underlying q is not needed but helpful to draw similarities with the other equilibration methods above.

(b) The equilibration estimator in [1] (which is labeled by η_{EQL}) uses linear edge functionals due to Ladeveze and Leguillon which consists of contributions associated to the nodes spanning the edge. By demanding the stronger condition $\mathrm{Res}_T(\varphi_z, q) = 0$, it is possible to solve local systems on node patches to calculate the contributions of z to its adjacent edges. It is possible to generate a global function q_{L} from these linear edge functionals (e.g., a Raviart-Thomas element of first order).

(c) The condition $\mathrm{Res}_T(1, q) = 0$ can be understood as a global consequence of the equilibration condition $\mathrm{div} q = -f$. Gauss theorem shows

$$\mathrm{Res}_T(1, q) = \int_T f\,dx + \int_{\partial T} q \cdot \nu\,ds = \int_T (f + \mathrm{div} q)\,dx = 0.$$

(d) The condition $\mathrm{Res}_T(1, q) = 0$ is clearly fullfilled by $q = q_{\mathrm{B}}$ constructed in Subsection 4.1. Therefore the edge fluxes of q_{B} can be used for the estimator described above and we label this by η_{EQB} in the numerical experiments. Since we have via (4.4) for $v = \phi_T$ and arguments from Subsection 4.1 that

$$\begin{aligned}\|\varkappa^{1/2}\nabla\phi_T\|_{L^2(T)} &= \frac{\mathrm{Res}_T(\phi_T, q)}{\|\varkappa^{1/2}\nabla\phi_T\|_{L^2(T)}}\\ &\leq \|\varkappa^{-1/2}(\sigma_h - q_{\mathrm{B}})\|_{L^2(T)} + 1/\pi \mathrm{osc}(f/\varkappa^{1/2}, T)\end{aligned}$$

the estimator η_{EQB} will be (locally) better than η_{B}.

(e) The problems in all mentioned methods to construct equilibrated fluxes locally look very similar and need the condition $\mathrm{Res}(\varphi_z) = 0$ for all $z \in \mathcal{K}$ for their solvability.

(f) Efficiency highly depends on the closeness of the equilibrated fluxes to the fluxes of the exact solution. An optimal choice (e.g. $\mu_E = \sigma \cdot \nu_E$) could even yield $|||e||| = \eta_{\mathrm{EQ}}$. Similarly $q = \sigma$ gives $\eta(q) = |||e|||$.

5. Error Estimation by Local Transmission Problems

This subsection is devoted to the description of η_{CF} which is called η_{L} in [22]. We use the partition of unity property of the nodal basis function to split up the residual

$$\mathrm{Res}(v) = \sum_{z \in \mathcal{N}} \mathrm{Res}(\varphi_z v).$$

Since $\mathrm{Res}(\varphi_z) = 0$ for $z \notin \partial\Omega$ there exist a unique solution $w_z \in W_z$ for the problem

$$\int_{\omega_z} \varkappa\varphi_z \nabla w_z \cdot \nabla v\,dx = \mathrm{Res}(\varphi_z v) \quad \text{for all } v \in W_z \tag{5.1}$$

with

$$W_z := \begin{cases} \left\{v \in H^1_{loc}(\omega_z) \,:\, \|(\varkappa\varphi_z)^{1/2}\nabla v\|_{L^2(\omega_z)} < \infty,\ v = 0 \text{ on } \partial\Omega \cap \partial\omega_z\right\} & \text{if } z \in \partial\Omega,\\ \left\{v \in H^1_{loc}(\omega_z) \,:\, \|(\varkappa\varphi_z)^{1/2}\nabla v\|_{L^2(\omega_z)} < \infty\right\} \setminus \mathbb{R} & \text{otherwise.}\end{cases}$$

Theorem 5.1. ([22]) *It holds*

$$|||e||| \leq \eta_{CF} := \left(\sum_{z \in \mathcal{N}} \|(\varkappa \varphi_z)^{1/2} \nabla w_z\|^2_{L^2(\omega_z)} \right)^{1/2}.$$

Proof. Since $\sum_{z \in \mathcal{N}} \varphi_z \equiv 1$ it follows

$$\begin{aligned} \mathrm{Res}(v) &= \sum_{z \in \mathcal{N}} \mathrm{Res}(\varphi_z v) \\ &= \sum_{z \in \mathcal{N}} \int_{\omega_z} \varkappa \varphi_z \nabla w_z \cdot \nabla v \, dx \\ &\leq \|(\varkappa \varphi_z)^{1/2} \nabla w_z\|_{L^2(\omega_z)} \|(\varkappa \varphi_z)^{1/2} \nabla v\|_{L^2(\omega_z)} \\ &\leq \eta_{\mathrm{CF}} \left(\sum_{z \in \mathcal{N}} \int_{\omega_z} \varphi_z |\varkappa^{1/2} \nabla v|^2 \right)^{1/2} \\ &= \eta_{\mathrm{CF}} |||v|||. \end{aligned}$$

This completes the proof of the theorem. □

Remark 5.1.

(a) The local problems (5.1) are solved approximately with a p-version of the finite element method on the node patch

$$\omega_z = \{T \in \mathcal{T} \, : \, z \in \partial T\}.$$

The numbers in our numerical experiments are obtained with fourth order polynomials.

(b) If $n = 2$ and $\varkappa = 1$ and $\mathcal{T}$ consists of right isosceles triangles, we have $\mathrm{C}_{\mathrm{eff}} \approx 2.36$ [22].

(c) Our η_{CF}-steered adaptive algorithm is based on the refinement indicator $\eta_{\mathrm{CF}}(T)$,

$$\eta_{\mathrm{CF}}(T) := \frac{1}{n+1} \sum_{z \in \mathcal{N} \cap T} \|(\varkappa \varphi_z)^{1/2} \nabla w_z\|^2_{L^2(\omega_z)} \quad \text{for each } T \in \mathcal{T}.$$

6. Adaptive Mesh Refinement

Automatic mesh refinement generates a sequence of meshes $\mathcal{T}_0$, $\mathcal{T}_1$, $\mathcal{T}_2$... by marking and refining elements according to a bulk criterion with parameter $0 \leq \Theta \leq 1$.

Algorithm A_Θ

(a) Start with a coarse mesh $\mathcal{T}_0$ and initialize $\ell = 0$.

(b) Compute the discrete solution u_h on the actual mesh $\mathcal{T}_\ell$ with N degrees of freedom. In case of inhomogenous Dirichlet boundary conditions u_D use its nodal interpolation $u_{D,h} = \sum_{z\in\mathcal{N}\setminus\mathcal{K}} u_D(z)\varphi_z$ for the discretisation.

(c) For xyz $\in$ {R, A1, A2, MP1, RT, MRT, B, MFEM, LS, LW, EQL, EQB, CF} compute $\eta_{\rm xyz}$ and the local refinement indicators $\eta_{\rm xyz}(T)$ for all $T \in \mathcal{T}_\ell$. In case of inhomogenous Dirichlet boundary conditions compute

$$\eta_D(E) := \varkappa_E^{1/2} h_E^{3/2} \|\partial_{\mathcal{E}}^2 u_D\|_{L^2(E)} \text{ for all } E \in \mathcal{E},\ E \subset \partial\Omega,$$

with the edgewise second derivative $\partial_{\mathcal{E}}^2 u_D$ of u_D along $\partial\Omega$. Substitute each $\eta_{xyz}(T)$ by $\eta_{xyz}(T)+\sum_{E\in\mathcal{E},\ E\subset(\partial T\cap\partial\Omega)} \eta_D(E)$. In case of nonzero oscillations we further substitute $\eta_{xyz}(T)$ by $\eta_{xyz}(T) + \operatorname{osc}(f, T)$ to control this quantity, too.

(d) The design of a minimal set $\mathcal{M}_\ell$ of elements to refine employs a greedy algorithm: Enumerate elements such that $\eta_{\rm xyz}(T_1) \geq \eta_{\rm xyz}(T_2) \geq ... \geq \eta_{\rm xyz}(T_{|\mathcal{T}|})$ where $|\mathcal{T}|$ is the total number of triangles in $\mathcal{T}_\ell$. Find the smallest index $k \in \mathbb{N}$, s.t.

$$\Theta \sum_{j=1}^{|\mathcal{T}|} \eta_{\rm xyz}(T_j) \leq \sum_{j=1}^{k} \eta_{\rm xyz}(T_j).$$

Set $\mathcal{M}_\ell := \{T_j \,:\, j = 1, .., k\}$.

(e) Generate a new triangulation $\mathcal{T}_{\ell+1}$ by *red*-refinement of elements in $\mathcal{M}_\ell$ and *red-green-blue*-refinement of further elements to avoid hanging nodes: Given $T \in \mathcal{T}$ and $\partial T = E_1 \cup E_2 \cup E_3$ where E_1 is the longest edge, a *red*-refinement of T is performed by dividing T into four congruent sub-triangles obtained by connecting the midpoints of the edges E_1, E_2 and E_3. A *blue*-refinement of T is performed by dividing T into three sub-triangles which are obtained by connecting the midpoint of E_1 with the opposite node and the midpoint of E_2 or E_3. A *green*-refinement of $T \in \mathcal{T}$ is performed by dividing T into two sub-triangles which are obtained by connecting the midpoint of the longest edge E_1 with the opposite node, cf. Figure 6.1. Update ℓ and go to (b).

Remark 6.1.

(a) The parameter Θ allows adaptive refinement for $\Theta = 1/2$ and uniform mesh refinement for $\Theta = 1$.

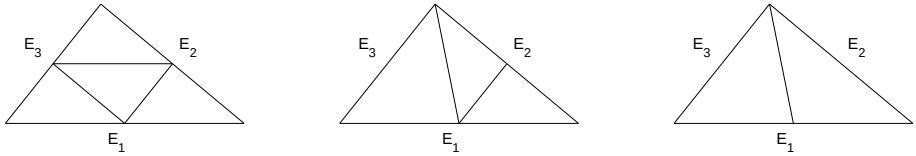

Fig. 6.1. Red-, blue-, and green-refinement of a triangle.

(b) There is remarkably little literature on a priori properties of adaptive algorithms [29, 41–43]; but their practical performance is actually very good. The convergence rates are usually reasonably improved.

(c) The finite element scheme and the adaptive algorithms were implemented in Matlab based on openffw [44] with direct solution of all linear systems of equations.

(d) In case of inhomogenous boundary conditions an estimator for the approximation error of the Dirichlet data u_D on the boundary was incorporated to control this quantity in the adaptive process, cf. [45] for details.

7. Numerical Examples

Example 7.1. ([22]) *Let $f \equiv 1$ and $\varkappa \equiv 1$ on the L-shaped domain*

$$\Omega := (-1,1)^2 \backslash [-1,0]^2,$$

$u \equiv 0$ on $\partial\Omega$. The coarsest triangulation consists of 12 triangles obtained by dividing each of the three quares into 4 congruent triangles. The exact solution is unknown, its energy norm $|||u|||^2 \approx 0.2140758036140825$ was obtained by Aitken extrapolation of solutions on uniform grids. The solution has a typical corner singularity at the origin.

For a uniform sequence of meshes $\mathcal{T}_0$, $\mathcal{T}_1$, $\mathcal{T}_2$,... generated by Algorithm A_Θ with $\Theta = 0$ we computed all error estimators and, using the approximated value for $|||u|||$ and Galerkin orthogonality, $|||e||| = |||u||| - |||u_h|||$. Figure 1.1 displays these quantities divided by $|||u|||$ and plotted against the number of degrees of freedom N corresponding to the particular triangulation. The logarithmic scaling of both axes results in a nearly constant slope of $-1/3$ for all graphs, which, in two dimensions, corresponds to an experimental convergence rate of $\alpha = 2/3$ as $h^\alpha \propto N^{-\alpha/2}$. This matches theoretical predictions for a domain with a reentrant corner and an interior angle of $3\pi/2$. Suppose a goal is a termination of the calculation with relative energy norm error $\leq 10\%$. Clearly, the error is below 10% for $\mathcal{T}_4$, but since, in general, $|||e|||$ is unknown, termination is to look on which level they cross the 10%-line. For example, η_{MP1} suggests stop at

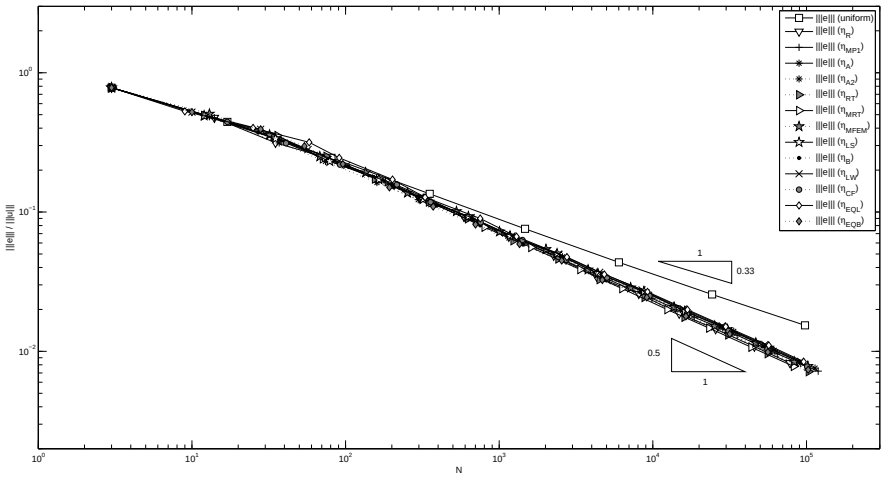

Fig. 7.1. Errors on adaptively generated meshes in Example 7.1.

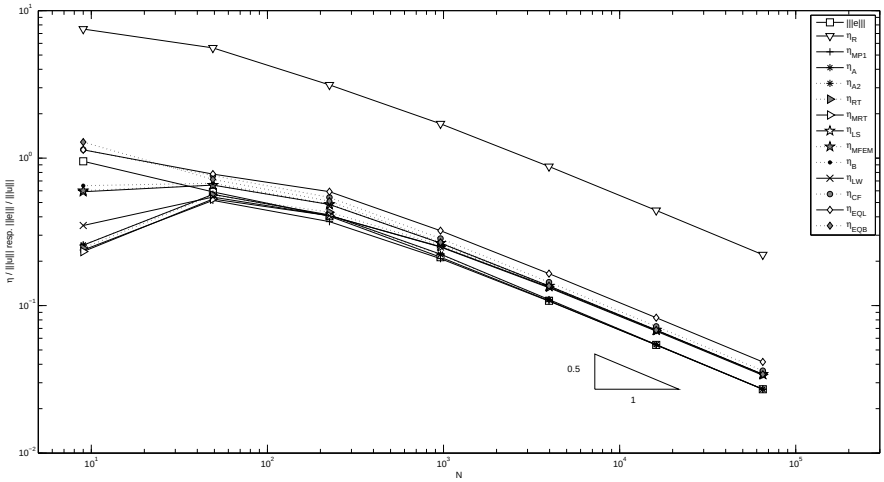

Fig. 7.2. Error and error estimators for uniform mesh refinement in Example 7.2.

$\mathcal{T}_4$ with 1473, η_{EQL} at $\mathcal{T}_5$ with 6017, and η_{R} at $\mathcal{T}_7$ with 97793 degrees of freedom. The other estimators are somewhere between η_{MP1} and η_{EQL}.

The experimental convergence rate of 2/3 can be improved by adaptive refinement. This is shown in Figure 7.1. Via algorithm $(A_{1/2})$ all estimators induce meshes with the optimal experimental convergence rate 1. The goal of 10% for the relative error is reached with 400 degrees of freedom instead of 800 for uniform refinement. However, there are slight differences: the meshes generated by the estimators based on Raviart-Thomas elements on the original triangulation and the standard-residual-based estimator η_{R} are the best, while η_{CF}, η_{EQL} and η_{LW} produce the worst meshes.

Example 7.2. ([19]) *We choose f according to the exact solution*

$$u = x(x-1)y(y-1)\exp(-100(x-1/2)^2 - (y-117)^2/10000)$$

of (1.1) *on* $\Omega = (0,1)^2$. *The oscillations are of higher order for small mesh-sizes.*

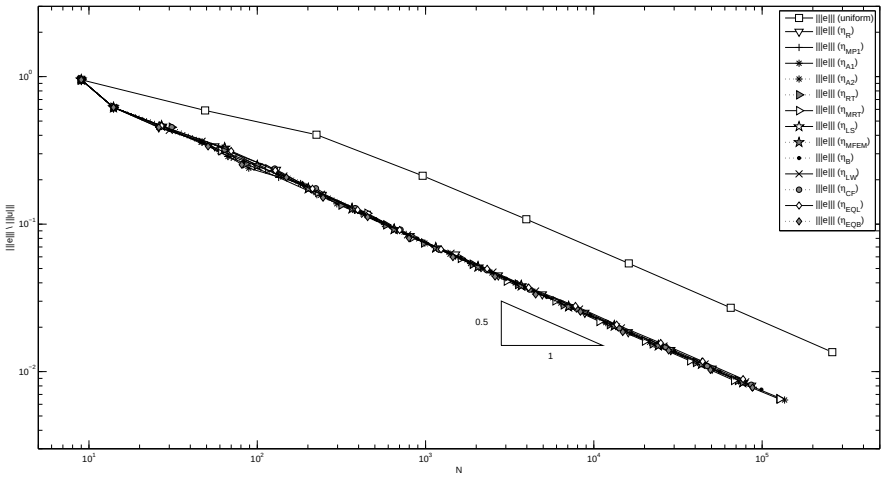

Fig. 7.3. Errors on adaptively generated meshes in Example 7.2.

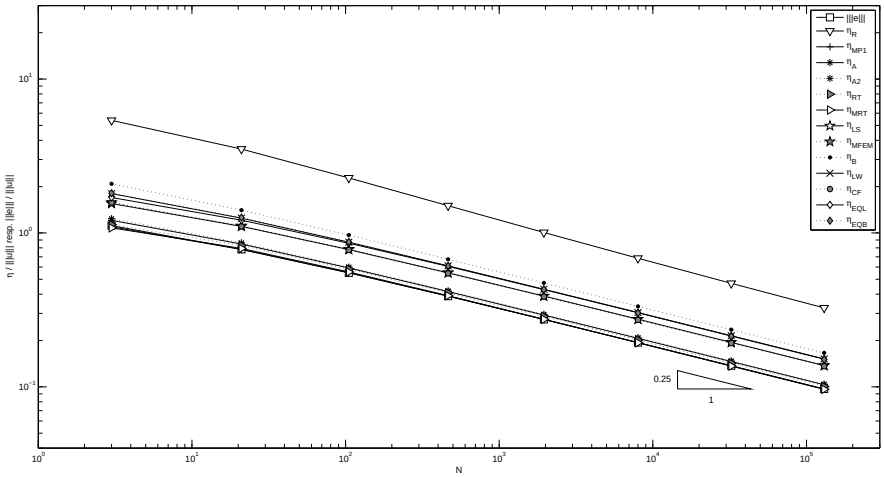

Fig. 7.4. Error and error estimators for uniform mesh refinement in Example 7.3.

Figure 7.2 shows the relative energy error and estimators on a sequence of uniformly refined meshes generated with algorithm (A_0) for $\Theta = 0$. Since $u \in H^2(\Omega)$, the optimal convergence rate is 1. Although this cannot be further improved by adaptive refinement, Figure 7.3 shows that it leads nonetheless to a significant error reduction. The error goal of 10% is reached with around 500 degrees of freedom while the uniform refinement needs about 4000 degrees of freedom. Again the meshes generated by $RT_0(\mathcal{T})$-based estimators generates the best meshes, while η_{EQL} produces the worst. The loss of reliability of η_{B}, η_{LW}, η_{MFEM} and η_{LS} in Figure 7.2 is due to the oscillations. The estimators η_{EQB}, η_{EQL} and η_{CF} are far less affected by this.

Example 7.3. ([43]) *The exact solution of* (1.1) *for* $f \equiv 1$ *and* $\varkappa \equiv 1$ *on the domain*

$$\Omega = \{(x, y) \in \mathbb{R}^2 \,:\, |x| + |y| < 1\} \backslash ([0, 1] \times \{0\})$$

is given (in polar coordinates) by $u(r, \phi) = r^{1/2} \sin(\phi/2) - 1/2 r^2 \sin^2 \phi$. *The coarsest triangulation consists of* 16 *triangles obtained by red-refining each of the four triangles in* Ω *minus the*

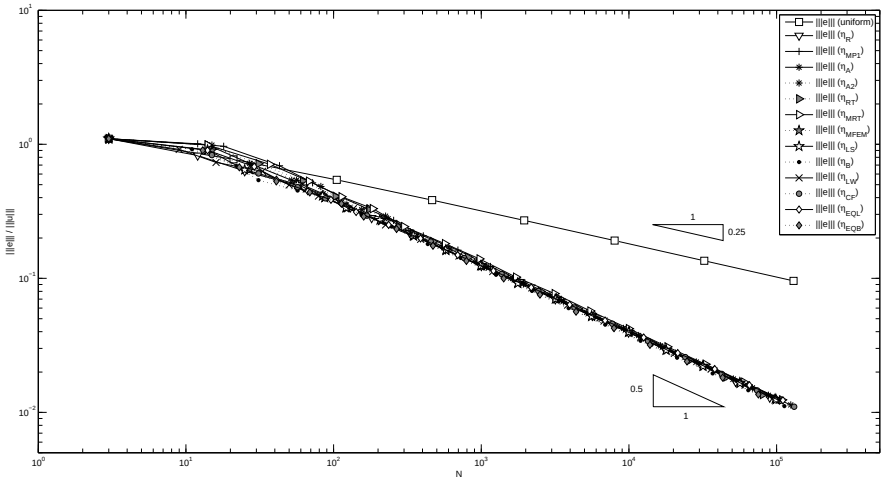

Fig. 7.5. Errors on adaptively generated meshes in Example 7.3.

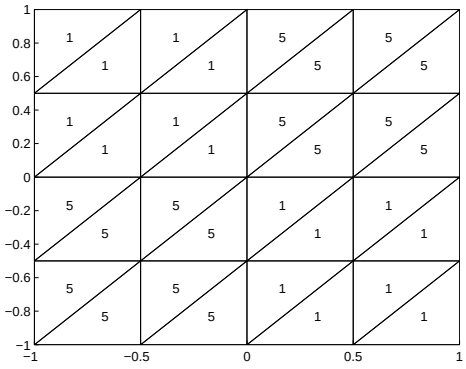

Fig. 7.6. Distribution of k on the initial triangulation in Example 7.4.

x- and y-axis. The solution has a typical corner or crack singularity [43].

Figure 7.4 shows the relative energy error and estimators on a sequence of uniformly refined meshes generated with an expected convergence rate of 1/2. This time the performance of η_{EQB} and η_{EQL} is very similar, which coincides with the observation that η_{B} is not as efficient as in the examples before. It is also remarkable that η_{MRT} is very accurate this time while in the examples before there was a little overestimation. The adaptively generated meshes improve the experimental convergence rate to the optimal value 1 as can be seen in Figure 7.5. This time the error goal of 10% is reached with around 100.000 degrees of freedom with uniform refinement and around 1000 degrees of freedom with adaptive refinement! The assessment of the meshes is the same as in the examples before, the meshes generated by η_{B} or η_{EQB} win by a narrow margin.

Example 7.4. ([19]) *We look on* $\Omega = (-1,1)^2$ *with* $f \equiv 0$ *and diffusion coefficients of* 1 *or* 5 *in each of the 4 sectors distributed as seen in Figure* 7.6. *The exact solution has the form (in polar coordinates)* $u(r,\phi) = r^\alpha\,(\beta\sin(\alpha\theta) + \gamma\cos(\alpha\theta))$ *with* $\alpha = 0.53544094560$. *The other*

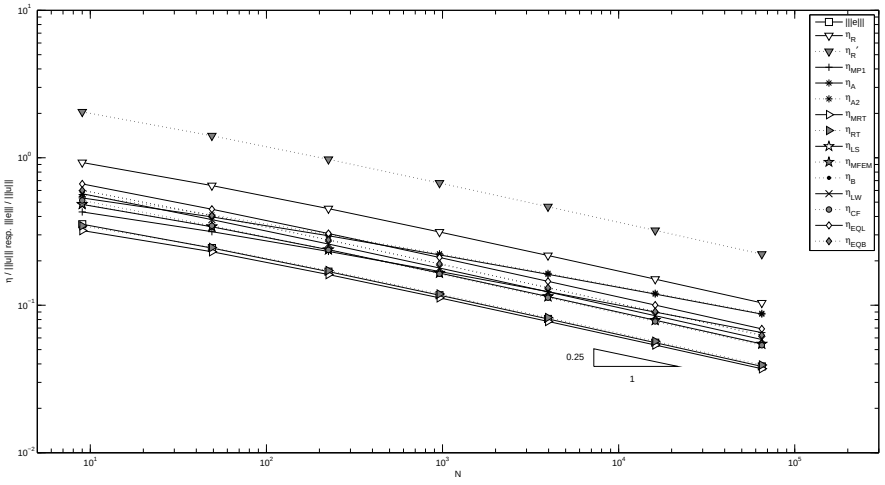

Fig. 7.7. Error and error estimators for uniform mesh refinement in Example 7.4.

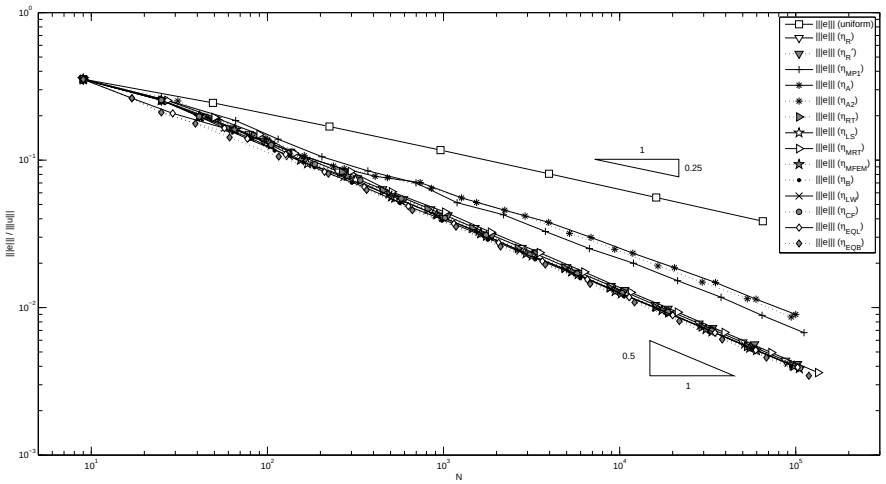

Fig. 7.8. Errors on adaptively generated meshes in Example 7.4.

coefficients β *and* γ *are chosen (differently on each sector of* Ω*) to solve* (1.1) *with the given data. The coarsest triangulation consists of* 16 *triangles achieved by red-refining each of the* 4 *sectors of the square. The solution has a singularity at the point* $(0, 0)$.

Figure 7.7 shows the results for uniform refinement with an experimental convergence rate of 1/2. The node based averaging estimators η_{A}, η_{A2} and also η_{MP1} fail in this example and do not recover the correct convergence rate. Again, η_{MRT} and η_{RT} give a good guess for the exact arror but are not a secured upper bound like the more laborous estimators η_{CF}, η_{LS}, η_{MFEM} and η_{LW}. The results for the adaptive refinements in Figure 7.8 show that the convergence rate again can be improved to the optimal value of 1 and underline the loss of efficiency for the node based averaging estimators. The meshes induced by η_{R} or η_{MRT} doesn't count to the best anymore and are defeated by most of the other estimators, predominantly the ones by η_{B} or η_{EQB}. For comparison we also included the estimator $\eta_{\mathrm{R}}\prime$ which is the explicit residual-based error estimator for $\varkappa \equiv 1$ to show what happens if the local diffusion coefficients are ignored. Since $\varkappa \leq 1$ in this example it holds $\eta_R \leq \eta_{\mathrm{R}}\prime$, but we also see that the adaptive meshes induced by $\eta_{\mathrm{R}}\prime$ are not as good as the ones induced by η_R.

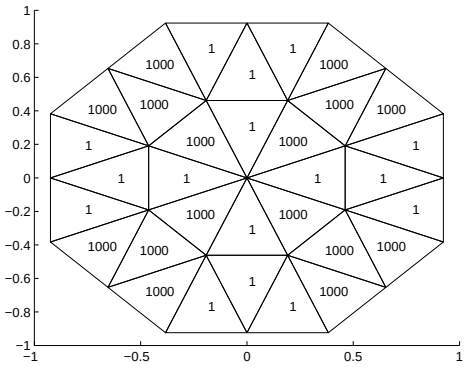

Fig. 7.9. Octagon and distribution of k on the initial triangulation in Example 7.5.

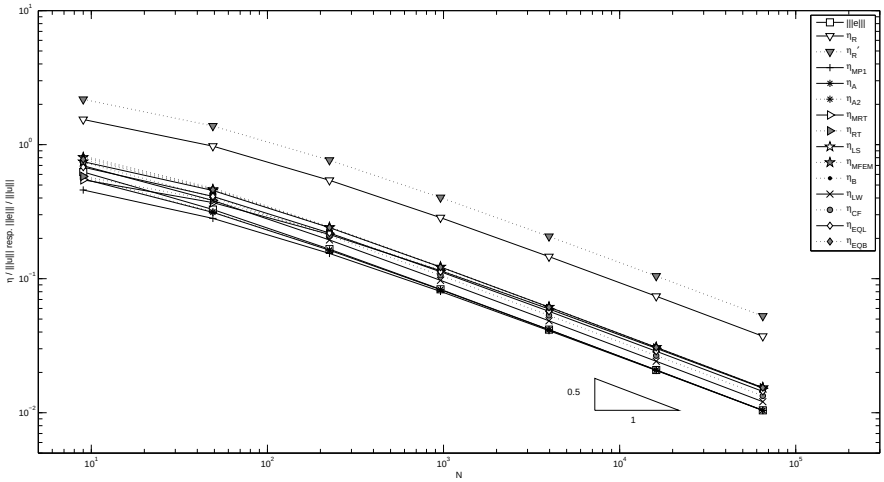

Fig. 7.10. Error and error estimators for uniform mesh refinement in Example 7.5.

Example 7.5. ([46]) *The diffusion coefficient* $\varkappa$ *assumes the values* 1 *and* 1000 *on the octagon*

$$\Omega = \mathrm{conv}\left\{\left(\cos\frac{(2j+1)\pi}{8}, \sin\frac{(2j+1)\pi}{8}\right),\ j=0,1,..,7\right\}$$

as depicted in Figure 7.9. *The remaining data of problem* (1.1) *are chosen to match the exact solution* $u(x,y) = (ax^2 - y^2)(ay^2 - x^2)/\varkappa$ *with* $a = \tan(3\pi/8)^2$. *The first derivatives of the solution are discontinuous at the interfaces while the flux* σ *is continuous. The coarsest triangulation consists of* 32 *triangles achieved by red-refining each of the* 8 *sectors of the octagon.*

Since the solution is very smooth we have the optimal convergence rate of 1 already for uniform refinement as seen in Figure 7.10. Surprisingly the estimator η_{LW} beats most other estimators and the node-based averaging estimators work again because the fluxes of the exact solution have no tangential jumps. Also remarkable is the apparent convergence of $\eta_{\mathrm{MRT}} \leq \eta_{\mathrm{LS}} \leq \eta_{\mathrm{MFEM}} \leq \eta_{\mathrm{B}}$ against each other. In this example η_{EQL} beats η_{EQB} for the first time,

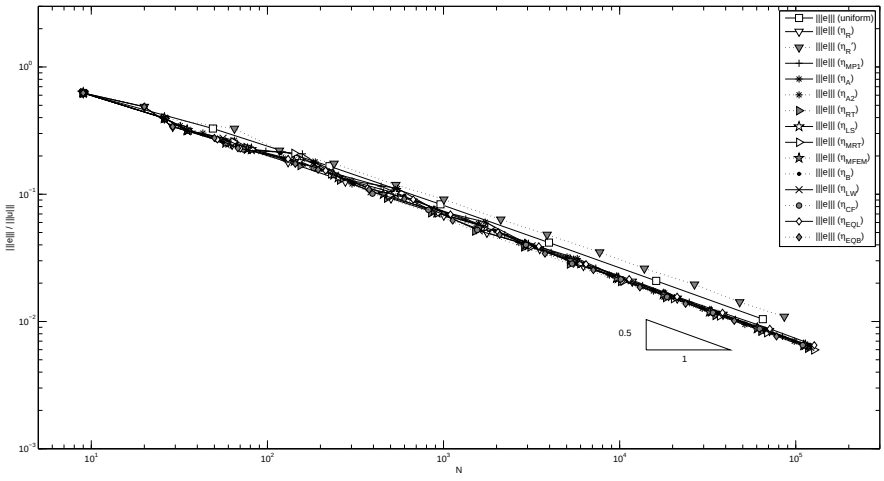

Fig. 7.11. Errors on adaptively generated meshes in Example 7.5.

but still loses against η_{CF} as in all other given examples. As before $\eta_{\mathrm{R}'}$ denotes the explicit residual-based error estimator for $\varkappa \equiv 1$ and the results for the adaptive meshes in Figure 7.11 show that $\eta_{\mathrm{R}'}$ is not worth anything. All other estimators produce proper meshes.

8. Comparison and Concluding Remarks

The theoretical and practical results of this paper support the following observations.

8.1. Explicit error estimators appropriate for effective mesh design

Adaptive mesh refinement may be steered by simple η_{R}-based refinement rules, but the best meshes were generated by η_{B} or its improvement η_{EQB}. However, it does not appear to be favourable to spend more computational time for more laborious refinement rules if the data are (relatively) smooth.

8.2. Experimental observations $\eta_{\mathbf{LW}} \leq \eta_{\mathbf{B}}$ and $\eta_{\mathbf{EQB}} \leq \eta_{\mathbf{EQL}}$

In most examples η_{EQB} dominates η_{EQL}, but the last examples shows that this holds not in general. In all our examples the equilibration estimator η_{LW} was at least as accurate as η_{B}.

8.3. Asymptotic equivalence of $\eta_{\mathbf{LS}} = \eta_{\mathbf{MFEM}}$

The least-square-estimator η_{LS} coincides with η_{MFEM} asymptotically as expected in Section 4.2.

8.4. Approximation of local problems

We found that fourth-order polynomials are sufficient enough to provide accurate approximations of the guaranteed upper bounds. However, for full reliability, this approximation error has to be controlled further. The numerical experiments in this paper leave this out and therefore are not fully reliable.

8.5. Robust averaging estimators

Node-based averaging estimators like η_{MP1} and η_{A} may fail in examples with discontinuous diffusion. Therefore they are not recommended for guaranteed error control. The special choices η_{A1} and η_{A2} performed similar. The estimators η_{RT} and η_{MRT} remain efficient also for discontinuous diffusion.

8.6. Robust error control via $\eta_{\mathbf{CF}}$, $\eta_{\mathbf{LS}}$, $\eta_{\mathbf{MFEM}}$ or $\eta_{\mathbf{LW}}$

The estimators η_{CF}, η_{LS} or η_{MFEM} and η_{LW} seem to be the most robust estimators and are recommended as a termination criterion for guaranteed error control. The residual-based estimator η_{R} is too coarse and not appropriate as termination criterion for guaranteed error control.

8.7. Accurate error control pays off

Averaging estimators might be a very good exact error guess but they do not guarantee to be an upper bound for the exact error to justify termination. On the other hand, relying only on cheap error estimators like η_{R} causes overkill refinements and might be more expensive than the computation of more laborious but sharper error estimators like the ones from Section 8.6. That's why it is is favourable to have a variety of estimators [7].

8.8. Recommendation in practise

If the reliability is highly important for absolute control of the error in the energy norm, it is recommended to employ η_{MFEM} or η_{LW}. The estimator η_{LS}, although asymptotically equivalent to η_{MFEM}, is not a guaranteed upper bound without proper constants and minimisation as in Repins majorant. However, the seperation of oscillations done for the derivation of η_{LS}, η_{MFEM}, η_{B} and η_{LW} in Section 4 should be also applicable to his approach. The implicit estimators η_{CF}, η_{EQB} and η_{EQL} require the exact solution of a local interface problem with PDEs which involve some extra error control (see 8.4).

For adaptive algorithms, the residual-based error estimates are sufficient (see 8.1).

In case of smooth data the approximation estimators η_{A1}, η_{A2} and η_{MP1} show an accurate energy error approximation. This is recommended to give an idea of the error, however without explicit computation of the reliability constants, there is no guaranteed error control. We do not recommend this for rigourous error estimation but we do enjoy the high accurary in many nice examples.

Acknowledgments. The work of the first author was partly supported by the WCU program through KOSEF (R31-2008-000-10049-0). Supported by DFG Research Center MATHEON.

References

[1] M. Ainsworth and J.T. Oden, A Posteriori Error Estimation in Finite Element Analysis, Wiley, 2000.

[2] R. Becker and R. Rannacher, A feed-back approach to error control in finite element methods: basic analysis and examples, *Numer. Math.*, **4**:4 (1996), 237–264.

[3] I. Babuška and T. Strouboulis, The Finite Element Method and its Reliability, Oxford University Press, 2001.

[4] K. Eriksson, D. Estep, P. Hansbo and C. Johnson, Introduction to adaptive methods for differential equations, *Acta Numerica*, (1995), 105158.

[5] R. Verfürth, A Review of A Posteriori Error Estimation and Adaptive Mesh Refinement Techniques, Wiley-Teubner, 1996.

[6] S. Repin, A Posteriori Estimates for Partial Differential Equations, volume 4 of *Radon Series on Computational and Applied Mathematics*, Walter de Gruyter, Berlin, 2008.

[7] C. Carstensen, S. Bartels and R. Klose, An experimental survey of a posteriori Courant finite element error control for the Poisson equation, *Adv. Comput. Math.*, **15**:1-4 (2001), 79–106.

[8] S.C. Brenner and L.R. Scott, The Mathematical Theory of Finite Element Methods, volume 15 of *Texts in Applied Mathematics*, Springer-Verlag, New York, 1994.

[9] P.G. Ciarlet, The Finite Element Method for Elliptic Problems, North-Holland Publishing Co., Amsterdam, 1978, Studies in Mathematics and its Applications, Vol. 4.

[10] I. Babuška and A. Miller, A feedback finite element method with a posteriori error estimations. Part I. The finite element method and some basic properties of the a posteriori error estimator, *Comput. Method. Appl. M.*, **61** (1987), 1–40.

[11] D. Braess, Finite Elements - Theory, fast Solvers, and Applications in Solid Mechanics, Cambridge University Press, New York, 2007.

[12] R. Rodriguez, Some remarks on zienkiewicz-zhu estimator, *Internat. J. Numer. Methods PDE*, **10** (1994), 625–635.

[13] R. Rodriguez, A posteriori error analysis in the finite element method, in: Finite element methods. 50 years of the courant element, conference held at the university of jyvaeskylae, finland, 1993.

[14] S.I. Repin, Two-sided estimates of deviation from exact solutions of uniformly elliptic equations, Proceedings of the St. Petersburg Mathematical Society, Vol. IX, volume 209 of *Amer. Math. Soc. Transl. Ser. 2*, pages 143–171, Providence, RI, 2003, Amer. Math. Soc.

[15] C. Carstensen, All first-order averaging techniques for a posteriori finite element error control on unstructured grids are effective and reliable, *Math. Comput.*, **73** (2004), 1153–1165.

[16] S. Repin, S. Sauter and A. Smolianski, A posteriori error estimation for the dirichlet problem with account of the error in the approximation of boundary conditions, *Computing*, **70**:3 (2003), 205–233.

[17] P. Raviart and J. Thomas, A mixed finite element method for 2-nd order elliptic problems, *Mathematical Aspects of Finite Element Methods, Lecture Notes in Math.*, **606** (1977), 292–315.

[18] C. Carstensen and C. Bahriawati, Three matlab implementations of the lowest-order Raviart-Thomas MFEM with a posteriori error control, *CMAM*, **5**:4 (2005), 333–361.

[19] R. Luce and B.I. Wohlmuth, A local a posteriori error estimator based on equilibrated fluxes, (2004).

[20] D. Braess and J. Schoeberl, Equilibrated residual error estimator for maxwell's equations, (2006).

[21] C. Bernardi and R. Verfürth, Adaptive finite element methods for elliptic equations with non-smooth coefficients, *Numer. Math.*, **85**:4 (2000), 579–608.

[22] C. Carstensen and S. Funken, Fully reliable localised error control in the fem, *SIAM J. Sci. Comput.*, **21**:4 (1999), 1465–1484 (electronic).

[23] M. Petzoldt, Regularity and error estimators for elliptic problems with discontinous coefficients, Dissertation, Weierstraß-Institut für Angewandte Analysis und Stochastik, 2001.

[24] C. Carstensen, Quasi-interpolation and a posteriori error analysis in finite element method, *M2AN Math. Model. Numer. Anal.*, **33**:6 (1999), 1187–1202.

[25] S.A. Funken, Beiträge zur a posteriori Fehlerabschätzung bei der numerischen Behandlung elliptischer partieller Differentialgleichungen - Theorie, Numerik und Anwendungen, Habilitation, Universitt Kiel, 2002.

[26] O. Zienkiewicz and J. Zhu, A simple error estimator and adaptive procedure for practical engineering analysis, *Int. J. Numer. Meth. Eng.*, **24** (1987), 337–357.

[27] C. Carstensen and R. Verfürth, Edge residuals dominate a posteriori error estimates for low order finite element methods, *SIAM J. Numer. Anal.*, **36**:5 (1999), 1571–1587.

[28] C. Carstensen, Merging the Bramble-Pasciak-Steinbach and the Crouzeix-Thomee criterion for H^1-stability of the L^2-projection onto finite element spaces, *Math. Comput.*, **71**:237 (2002), 157–163.

[29] W. Dörfler and R.H. Nochetto, Small data oscillation implies the saturation assumption, *Numer. Math.*, **91**:1 (2002), 1–12.

[30] R.H. Nochetto, Removing the saturation assumption in a posteriori error analysis, *Istit. Lombardo Accad. Sci. Lett. Rend. A*, **127**:1 (1993), 67–82 (1994).

[31] C. Carstensen and S. Bartels, Each averaging technique yields reliable a posteriori error control in FEM on unstructured grids part I: Low order conforming, nonconforming, and mixed FEM, *Math. Comput.*, **71**:239 (2002), 945–969.

[32] C. Carstensen and S. Bartels, Each averaging technique yields reliable a posteriori error control in FEM on unstructured grids. Part II: Higher order FEM, *Math. Comput.*, **71**:239 (2002), 971–994.

[33] C. Carstensen and S. Funken, Averaging technique for FE-a posteriori error control in elasticity. Part I: Conforming FEM; Part II: λ-independent estimates; Part III: Locking-free nonconforming FEM, *Comput. Method. Appl. M.*, **190-191** (2001).

[34] C. Carstensen and S. Funken, A posteriori error control in low-order finite element discretisations of incompressible stationary flow problems, *Math. Comput.*, **70**:236 (2001), 1353–1381.

[35] C. Carstensen and J. Alberty, Averaging techniques for reliable a posteriori FE-error control in elastoplasticity with hardening, *Comput. Method. Appl. M.*, **192** (2003), 1435–1450.

[36] C. Carstensen and S. Bartels, Averaging techniques yield reliable a posteriori finite element error

control for obstacle problems, *Numer. Math.*, **99**:2 (2004), 225–249.

[37] P. Ladeveze and D. Leguillon, Error estimate procedure in the finite element method and applications, *SIAM J. Numer. Anal.*, **20**:3 (1983), 485–509.

[38] M. Ainsworth and J.T. Oden, A posteriori error estimators for second order elliptic systems. I. Theoretical foundations and a posteriori error analysis, *Comput. Math. Appl.*, **25**:2 (1993), 101–113.

[39] M. Ainsworth and J.T. Oden, A posteriori error estimators for second order elliptic systems. II. An optimal order process for calculating self-equilibrating fluxes, *Comput. Math. Appl.*, **26**:9 (1993), 75–87.

[40] M. Ainsworth and J.T. Oden, A unified approach to a posteriori error estimation using element residual methods, *Numer. Math.*, **65**:1 (1993), 23–50.

[41] W. Doerfler, A convergent adaptive algorithm for Poissons equation, *SIAM J. Numer. Anal.*, **33**:3 (1996), 1106–1124.

[42] Morin, P. and Nochetto, R.H. and Siebert, K.G., Data oscillation and convergence of adaptive FEM, *SIAM J. Numer. Anal.*, **38**:2 (2000), 466–488.

[43] P. Morin, R.H. Nochetto and K.G. Siebert, Local problems on stars: a posteriori error estimators, convergence, and performance, *Math. Comput.*, **72**:243 (2003), 1067–1097 (electronic).

[44] A. Byfut, J. Gedicke, D. Günther, H. Mellmann, J. Reininghaus and S. Wiedemann, FFW Documentation, `http://openffw.googlecode.com/svn/homepage/index.htm`.

[45] C. Carstensen, G. Dolzmann and S. Bartels, Inhomogeneous Dirichlet conditions in a priori and a posteriori finite element error anylysis, *Numer. Math.*, **99**:1 (2004), 1–24.

[46] R.H. Hoppe and B. Wohlmuth, Element-oriented and edge-oriented local error estimators for nonconforming finite element methods, *M2AN, Modélisation Math. Anal. Numér.*, **30** (1996), 237–263.